Chemical Engineering Journal 100 (2004) 119–127

Chemical Engineering Journal

www.elsevier.com/locate/cej

A comparison of a pseudo-homogeneous non-equilibrium model and a three-phase non-equilibrium model for catalytic distillation

Yuxiang Zheng, Flora T.T. Ng*, Garry L. Rempel

Department of Chemical Engineering, University of Waterloo, 200 University Avenue West, Waterloo, Ont., Canada N2L 3G1

Received 29 July 2003; accepted 2 January 2004

Abstract

A comparison of computer simulation results of catalytic distillation (CD) obtained from a three-phase non-equilibrium model and a pseudo-homogeneous non-equilibrium model was performed. Simulations were carried out on the CD processes for the production of ethyl cellosolve (EC) and diacetone alcohol (DAA) using both the pseudo-homogeneous non-equilibrium model and the three-phase non-equilibrium model. Similar results for the synthesis of EC were obtained using these two models. However, only the three-phase non-equilibrium model could adequately describe the CD process for the aldol condensation of acetone (Ac) at low reflux flow rates. Hence our results suggest that for a reaction system that is kinetically controlled, a pseudo-homogeneous non-equilibrium may adequately simulate the temperature profile, yield and selectivity for a CD process. However, for a CD process that is sensitive to solid–liquid mass transfer, the three-phase non-equilibrium model is required.

Keywords: Catalytic distillation; Non-equilibrium model; Three-phase model; Ethyl cellosolve; Diacetone alcohol; Pseudo-homogeneous model

1. Introduction

The combination of reaction and separation into a single unit provides many advantages, such as high selectivity and yield, energy saving, lower capital investment and simpler operation. One of the most common methods of in situ separation of products from reactants is a catalytic distillation (CD) process that combines a heterogeneous catalytic reaction and distillation into a single unit operation. Recently there is considerable academic and industrial interest in the CD technology. The total numbers of publications and patents are increasing every year [1]. The most recent review of CD is by Ng and Rempel [2].

To design and optimize a CD process, a theoretical model is important in obtaining the composition and temperature profiles along the column. Many CD simulation results are based on the equilibrium model for conventional distillation processes [3–5]. However, the column rarely operates at equilibrium in actual operation. So the concept of stage efficiency is generally introduced to correct the difference between equilibrium and real stages for trays. For a packed column, the equilibrium model requires the values of the height equivalent theoretical plate (HETP). In reality, however, the stage efficiency and HETP cannot be predicted reliably for a multicomponent mixture [6], especially in the processes of chemical reactions [7]. Since it is the rate for transports or reaction and not the equilibrium that controls the yield and selectivity for a CD process, a non-equilibrium model would be more appropriate for the simulation of a CD process. Taylor and Krishna [8] have given a comprehensive review of the modelling of reactive/catalytic distillation.

Although simulation results have been published for various CD columns using a non-equilibrium model, most of them are based on the pseudo-homogeneous (two-phase) non-equilibrium model [9–13]. A CD process is more complex than a homogeneous reactive distillation process due to the existence of the heterogeneous reactions. It appears that a three-phase non-equilibrium model is more appropriate for the simulation of CD because there are concentration and temperature gradients between the liquid and solid phases in most reaction systems. Sundmacher and Hoffmann [14] employed the catalyst effectiveness factor to account for diffusion and reaction inside the catalyst. Although the heat transfer between phases was ignored in their process modelling, they concluded that a three-phase model is absolutely necessary for a CD process. Higler et al. [15] used the dusty fluid model to take into account mass transport inside the

* Corresponding author. Tel.: +1-519-888-4567x3979; fax: +1-519-746-4979.
E-mail address: fttng@cape.uwaterloo.ca (F.T.T. Ng).

1385-8947/$ – see front matter © 2004 Elsevier B.V. All rights reserved.
doi:10.1016/j.cej.2004.01.015

Nomenclature

a	effective interfacial area (m^2 section^{-1})
a_t	specific surface area of packing ($m^2\,m^{-3}$)
a_w	wetted area ($m^2\,m^{-3}$)
A_{12}, A_{21}	interaction energy parameters (kJ kmol^{-1})
c	molar concentration (kmol m^{-3})
C	total number of components
C_P	heat capacity (kJ kmol^{-1} K^{-1})
d_p	equivalent diameter of packing (m)
D	binary diffusion coefficient ($m^2\,s^{-1}$)
e	heat transfer rate (kJ s^{-1})
f	feed rate of component (kmol s^{-1})
g	acceleration of gravity
G	weight of catalyst in section j (kg)
h	heat transfer coefficient (kJ $m^{-2}\,s^{-1}$ K^{-1})
H	mole enthalpy (kJ kmol^{-1})
J	J factor
k	EC formation forward rate constant (min^{-1})
k	multicomponent mass transfer coefficient (kmol $m^{-2}\,s^{-1}$)
k_1	DAA formation forward rate constant (l mol^{-1} min^{-1})
k_{-1}	DAA formation reversible rate constant (min^{-1})
k_2	MO and water formation rate constant (mol l^{-1} min^{-1})
K	equilibrium ratio
l	liquid component flow rate (kmol s^{-1})
Le	Lewis number ($\lambda M\rho^{-1}C_P^{-1}D^{-1}$)
M	molecular weight (kg kmol^{-1})
N	mass transfer rate (kmol s^{-1})
P	pressure (kPa)
Q	heat duty (kJ s^{-1})
r	macro kinetic rate (kmol (kg cat)$^{-1}$ s^{-1})
R	universal gas constant (8.314 kJ kmol^{-1} K^{-1})
Sc	Schmidt number ($\mu\rho^{-1}D^{-1}$)
T	absolute temperature (K)
v	vapour component flow rate (kmol s^{-1})
W	mass flow rate (kg $m^{-2}\,s^{-1}$)
x	liquid composition, mole fraction
y	vapour composition, mole fraction
Z	packed height of each section

Greek letters

δ	Kronecker delta, equal to 1 if $i = j$; otherwise equal to 0
ε	thermodynamic factors
γ	liquid-phase activity coefficient
Γ	thermodynamic matrix
κ	binary mass transfer coefficient (kmol $m^{-2}\,s^{-1}$)
λ	conductivity coefficient (kJ $m^{-1}\,s^{-1}$ K^{-1})
μ	viscosity (Pa s)
ν	stoichiometric coefficient
ρ	density (kg m^{-3})
σ	surface tension (N m^{-1})
σ_c	critical surface tension of packing (N m^{-1})

Subscripts

av	average value
C	number of components
D	mass transfer
H	energy transfer
i	component index
j	section index
k	alternative component index
m	property of mixture

Superscripts

I	vapor–liquid interface
L	liquid phase
LF	liquid feed
r	reaction
S	catalyst or solid phase
V	vapour phase
VF	vapour feed

catalyst. However, the authors stated that good estimation methods are absent for the calculation of the diffusion coefficients and the nonideal thermodynamic behaviour inside a catalyst. They found that both the pseudo-homogeneous and dusty fluid models could describe the CD process for the production of *tert*-amyl methyl ether (TAME) [15,16]. However, the difference between the pseudo-homogeneous and dusty fluid models is substantial for the methyl *tert*-butyl ether (MTBE). They suggested that the MTBE process is relatively sensitive to mass transfer resistances, whereas the TAME process is not.

A three-phase non-equilibrium model was developed by our group [17–20], which assumed the reaction rate and the mass transfer rate through the solid–liquid interface to be equal. In addition, the reaction heat was assumed to be equal to the heat transfer rate between the solid and liquid phases. The effect of multicomponent mass and heat transfer between phases was taken into account according to the Maxwell–Stefan equations [19,20]. In our three-phase non-equilibrium model, experimental macrokinetics was used in the calculation of reaction rates, which avoids the inherent difficulties in the estimation of the diffusion inside the catalyst particle as required in the dusty fluid model developed by Higler et al. [15]. We have already shown that our three-phase non-equilibrium model provides excellent predictions of the temperature profile and the yields and selectivities for the aldol condensation of acetone (Ac) [19]. However, we did not carry out simulation using the pseudo-homogeneous non-equilibrium model which is simpler but ignores the mass transfer between the liquid and

solid phases which are dependent on the operating conditions for the CD process and also the method used for packing the catalyst in the reaction zone. The objective of this paper is to ascertain when a pseudo-homogeneous non-equilibrium model or a three-phase non-equilibrium model should be used for the simulation of a CD process. This paper will compare the simulation results obtained from using a pseudo-homogeneous non-equilibrium model and a three-phase non-equilibrium model for two CD processes, namely, the synthesis of ethyl cellosolve (EC) and diacetone alcohol (DAA). Simulations results for the CD processes will also be compared with experimental data. Results of this study provide some insight on choosing between the pseudo-homogeneous non-equilibrium and the three-phase non-equilibrium model for the simulation of CD processes and will be discussed.

2. Mathematical models

A physical model of a three-phase non-equilibrium section is shown in Fig. 1. Based on the control volumes for vapour phase, liquid phase and solid (catalyst) phase, the mass and energy balances are developed separately for a steady-state process. Fig. 2 is a physical model of a pseudo-homogeneous non-equilibrium section. The mass and energy balances are developed for each of vapour and liquid phases. The assumptions are summarized in Table 1 for each model. The most important difference between these two models is the consideration of the temperature and concentration gradients between the liquid bulk and catalyst surface. Table 2 lists the model equations for each model.

In these models the multicomponent mass transfer coefficients are computed using the generalized Maxwell–Stefan equations for multicomponent transport in a film [21], which can be derived directly from the binary mass transfer coefficients as follows.

Vapor phase:

$$[k_{ik}^{\mathrm{V}}] = [B_{ik}^{\mathrm{V}}]^{-1} \tag{1}$$

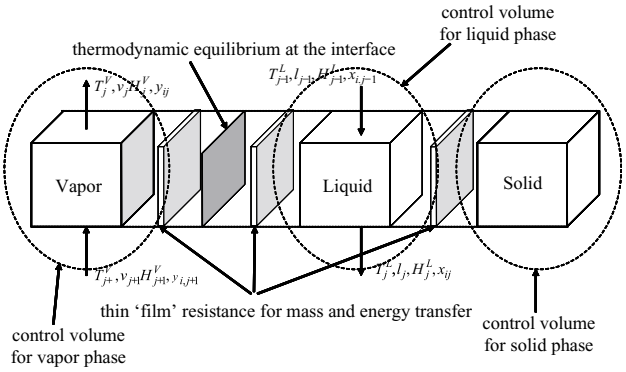

Fig. 1. A typical section of a three-phase non-equilibrium model.

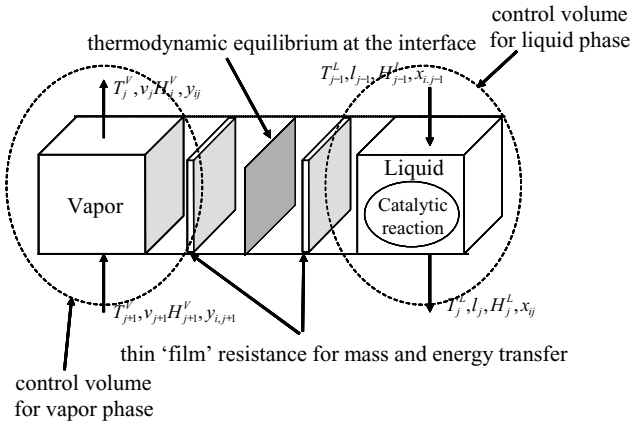

Fig. 2. A typical section of a pseudo-homogeneous non-equilibrium model.

Liquid phase:

$$[k_{ik}^{\mathrm{L}}] = [B_{ik}^{\mathrm{L}}]^{-1}[\Gamma_{ik}] \tag{2}$$

where

$$B_{ii}^{\mathrm{V}} = \frac{y_i}{\kappa_{ic}^{\mathrm{V}}} + \sum_{k=1_{k\neq i}}^{c} \frac{y_k}{\kappa_{ik}^{\mathrm{V}}}, \quad i = 1, 2, \ldots, C-1 \tag{3}$$

$$B_{ik}^{\mathrm{V}} = -y_i \left(\frac{1}{\kappa_{ik}^{\mathrm{V}}} - \frac{1}{\kappa_{ic}^{\mathrm{V}}} \right), \quad i \neq k = 1, 2, \ldots, C-1 \tag{4}$$

Table 1
Assumptions used in model development

Pseudo-homogeneous non-equilibrium model	Three-phase non-equilibrium model
Operation reaches steady-state	Operation reaches steady-state
System reaches mechanical equilibrium	System reaches mechanical equilibrium
The interface of vapor–liquid is uniform and in thermodynamic equilibrium	The interface of vapor–liquid is uniform and in thermodynamic equilibrium
The vapour and liquid bulk on each side of it are mixed perfectly	The vapour and liquid bulk on each side of it are mixed perfectly
The mixing effect can be neglected	The mixing effect can be neglected
The liquid and vapour phases in condenser and reboiler are still considered to be at equilibrium	The liquid and vapour phases in condenser and reboiler are still considered to be at equilibrium
Reactions only take place in the liquid bulk	Reactions only take place in the catalyst surface
The temperature and concentration gradients between liquid bulk and catalyst surface are ignored	

Table 2
Comparison of the pseudo-homogeneous non-equilibrium and three-phase non-equilibrium model equations

Pseudo-homogeneous non-equilibrium model	Three-phase non-equilibrium model
Mass balances for the vapour phase $v_{ij} - v_{i,j+1} - f_{ij}^{V} + N_{ij}^{V} = 0$	Mass balances for the vapour phase $v_{ij} - v_{i,j+1} - f_{ij}^{V} + N_{ij}^{V} = 0$
Mass balances for the liquid phase $l_{ij} - l_{i,j-1} - f_{ij}^{L} - N_{ij}^{L} - v_i r_{ij} G_j = 0$	Mass balances for the liquid phase $l_{ij} - l_{i,j-1} - f_{ij}^{L} - N_{ij}^{L} - N_{ij}^{S} = 0$
	Mass balances for the solid phase $N_{ij}^{S} - v_i r_{ij} G_j = 0$
Heat balance for the vapour phase $\sum_{i=1}^{C} v_{ij} H_j^{V} - \sum_{i=1}^{C} v_{i,j+1} H_{j+1}^{V} - \sum_{i=1}^{C} f_{ij}^{V} H_j^{VF} + e_j^{V} = 0$	Heat balance for the vapour phase $\sum_{i=1}^{C} v_{ij} H_j^{V} - \sum_{i=1}^{C} v_{i,j+1} H_{j+1}^{V} - \sum_{i=1}^{C} f_{ij}^{V} H_j^{VF} + e_j^{V} = 0$
Heat balance for the liquid phase $\sum_{i=1}^{C} l_{ij} H_j^{L} - \sum_{i=1}^{C} l_{i,j-1} H_{j-1}^{L} - \sum_{i=1}^{C} f_{ij}^{L} H_j^{LF} - e_j^{L} - Q_j^{r} = 0$	Heat balance for the liquid phase $\sum_{i=1}^{C} l_{ij} H_j^{L} - \sum_{i=1}^{C} l_{i,j-1} H_{j-1}^{L} - \sum_{i=1}^{C} f_{ij}^{L} H_j^{LF} - e_j^{L} - e_j^{S} = 0$ Heat balance for the solid phase $e_j^{S} - Q_j^{r} = 0$
Mass transfer in the vapour phase $N_{ij}^{V} = \sum_{k=1}^{C-1} k_{ikj}^{V} a_j (y_{kj} - y_{kj}^{I}) + y_{ij} \sum_{k=1}^{C} N_{kj}^{V}$	Mass transfer in the vapour phase $N_{ij}^{V} = \sum_{k=1}^{C-1} k_{ikj}^{V} a_j (y_{kj} - y_{kj}^{I}) + y_{ij} \sum_{k=1}^{C} N_{kj}^{V}$
Mass transfer in the liquid phase $N_{ij}^{L} = \sum_{k=1}^{C-1} k_{ikj}^{L} a_j (x_{kj}^{I} - x_{kj}) + x_{ij} \sum_{k=1}^{C} N_{kj}^{L}$	Mass transfer in the liquid phase $N_{ij}^{L} = \sum_{k=1}^{C-1} k_{ikj}^{L} a_j (x_{kj}^{I} - x_{kj}) + x_{ij} \sum_{k=1}^{C} N_{kj}^{L}$ Mass transfer in the solid phase $N_{ij}^{S} = \sum_{k=1}^{C-1} k_{ikj}^{S} a_j^{S} (x_{kj} - x_{kj}^{S}) + x_{ij} \sum_{k=1}^{C} N_{kj}^{S}$
Heat transfer in the vapour phase $e_j^{V} = h_j^{V} a_j \frac{\varepsilon_j^{V}}{\exp \varepsilon_j^{V} - 1} (T_j^{V} - T_j^{I}) + \sum_{k=1}^{C} N_{kj}^{V} H_{kj}^{V}$	Heat transfer in the vapour phase $e_j^{V} = h_j^{V} a_j \frac{\varepsilon_j^{V}}{\exp \varepsilon_j^{V} - 1} (T_j^{V} - T_j^{I}) + \sum_{k=1}^{C} N_{kj}^{V} H_{kj}^{V}$
	Heat transfer in the liquid phase $e_j^{L} = h_j^{L} a_j (T_j^{I} - T_j^{L}) + \sum_{k=1}^{C} N_{kj}^{L} H_{kj}^{L}$
Heat transfer in the liquid phase $e_j^{L} = h_j^{L} a_j (T_j^{I} - T_j^{L}) + \sum_{k=1}^{C} N_{kj}^{L} H_{kj}^{L}$	Heat transfer in the solid phase $e_j^{S} = h_j^{S} a_j^{S} (T_j^{L} - T_j^{S}) + \sum_{k=1}^{C} N_{kj}^{S} H_{kj}^{L}$
Phase equilibrium at the interface $K_{ij}^{I} x_{ij}^{I} - y_{ij}^{I} = 0$	Phase equilibrium at the interface $K_{ij}^{I} x_{ij}^{I} - y_{ij}^{I} = 0$
Relationship between vapour and liquid mass transfer $N_{ij}^{V} - N_{ij}^{L} = 0$	Relationship between vapour and liquid mass transfer $N_{ij}^{V} - N_{ij}^{L} = 0$
Relationship between vapour and liquid heat transfer $e_j^{V} - e_j^{L} = 0$	Relationship between vapour and liquid heat transfer $e_j^{V} - e_j^{L} = 0$

and

$$\Gamma_{ik} = \delta_{ik} + x_i \frac{\partial \ln \gamma_i}{\partial x_k}, \quad i, k = 1, 2, \ldots, C-1 \tag{5}$$

$$B_{ii}^{L} = \frac{x_i}{\kappa_{ik}^{L}} + \sum_{k=1_{k \neq i}}^{c} \frac{x_k}{\kappa_{ik}^{L}}, \quad i = 1, 2, \ldots, C-1 \tag{6}$$

$$B_{ik}^{L} = -x_i \left(\frac{1}{\kappa_{ik}^{L}} - \frac{1}{\kappa_{ic}^{L}} \right), \quad i \neq k = 1, 2, \ldots, C-1 \tag{7}$$

The binary mass transfer coefficients for general packing column have been developed by Onda et al. [22]. For the rectifying and stripping sections, the vapour film mass transfer coefficients are

$$\kappa_{ik}^{V} = \alpha \left(\frac{W^{V}}{a_t \mu_m^{V}} \right)^{0.7} (Sc_{ik}^{V})^{1/3} (a_t d_p)^{-2} \left(\frac{a_t D_{ik}^{V} P}{RT^{V}} \right) \tag{8}$$

where α is 2.0 for our small packings [22], and the liquid film mass transfer coefficients are calculated by

$$\kappa_{ik}^{L} = 0.0051 \left(\frac{W^{L}}{a_t \mu_m^{L}} \right)^{2/3} (Sc_{ik}^{L})^{-0.5} (a_t d_p)^{0.4} \left(\frac{g \mu_m^{L}}{\rho_m^{L}} \right)^{1/3} \rho_m^{L} \tag{9}$$

where a_w is the wetted area of packing and can be estimated by

$$a_w = a_t \left\{ 1 - \exp \left[-1.45 \left(\frac{W^{L}}{a_t \mu_m^{L}} \right)^{0.1} \left(\frac{a_t (W^{L})^2}{g \rho_m^{L\,2}} \right)^{-0.05} \times \left(\frac{(W^{L})^2}{a_t \sigma_m \rho_m^{L}} \right)^{0.2} \left(\frac{\sigma_m}{\sigma_c} \right)^{-0.75} \right] \right\} \tag{10}$$

In addition, the effective interfacial area is evaluated by the empirical correlation developed by Bravo and Fair [23]:

$$a = 0.498 a_t \left(\frac{\sigma_m^{0.5}}{Z^{0.4}} \right) \left(\frac{6 W^{V} \mu_m^{L} W^{L}}{a_t \mu_m^{V} \rho_m^{L} \sigma_m g} \right)^{0.392} \tag{11}$$

The binary mass transfer coefficients for the reactive section packed with the fiberglass bags and wrapped with demister wire have been developed by Zheng and Xu [24]. The vapour film mass transfer coefficients are given by

$$\kappa_{ik}^{V} a = 1.072 \times 10^{-3} \frac{a_t D_{ik}^{V}}{d_p R T^{V}} \left(\frac{4 W^{V}}{a_t \mu_m^{V}} \right)^{0.92} \times \left(\frac{4 W^{L}}{a_t \mu_m^{L}} \right)^{0.24} (Sc_{ik}^{V})^{0.5} \tag{12}$$

Table 3
Kinetic rate constants for acetone dimerization determined by Podrebarac et al. [28]

Catalyst[a]	k_1 ($M^{-1}\,min^{-1}$)	k_1/k_{-1} (M^{-1})	k_2 ($M\,min^{-1}$)
I	$3.12 \times 10^{-4} \exp(-0.9748 c_{H_2O})$	1.86×10^{-3}	$9.60 \times 10^{-4} \exp(-1.7161 c_{H_2O})$
II	$2.95 \times 10^{-4} \exp(-0.9748 c_{H_2O})$	1.86×10^{-3}	$1.42 \times 10^{-3} \exp(-1.7161 c_{H_2O})$

[a] Catalysts I and II are IRA-900 ion exchange resins exchanged with NaOH for 24 and 3 h resulting in 0.49 and 0.45 mmol $OH^-\,ml^{-1}$ catalyst loadings, respectively.

the liquid film mass transfer coefficients are obtained by

$$\kappa_{ik}^{L} a = 0.149 \frac{a_t D_{ik}^{L}}{d_p} \left(\frac{4W^{L}}{a_t \mu_m^{L}} \right)^{0.3} (Sc_{ik}^{L})^{0.5} \quad (13)$$

and the liquid–solid mass transfer coefficients are evaluated by

$$\kappa_{ik}^{S} a = 0.586 \frac{a_t W^{L}}{\rho_m^{L}} \left(\frac{4W^{V}}{a_t \mu_m^{V}} \right)^{-0.27} \left(\frac{4W^{L}}{a_t \mu_m^{L}} \right)^{-0.28} (Sc_{ik}^{L})^{-2/3} \quad (14)$$

The heat transfer coefficients h_j are estimated based on the Chilton–Colburn analogy, namely, $J_H = J_D$ [25], therefore

$$h^{V} = k_{av}^{V} C_{pm}^{V} (Le^{V})^{2/3} \quad (15)$$

for the vapour phase and

$$h^{L} = k_{av}^{L} C_{pm}^{L} (Le^{L})^{1/2} \quad (16)$$

for the liquid phase.

The CD processes for the aldol condensation of Ac [26,27] and the synthesis of EC from ethanol (EA) and ethylene oxide (EO) were chosen as examples. A simplified reaction scheme for the aldol condensation of Ac can be represented by the equation:

$$Ac \underset{k_{-1}}{\overset{k_1}{\rightleftharpoons}} DAA \xrightarrow{k_2} MO + H_2O \quad (17)$$

The kinetic data for the aldol condensation of Ac is taken from the data of Podrebarac et al. [28] as follows:

$$r_{DAA} = k_1 c_{Ac}^2 - (k_{-1} + k_2) c_{DAA} \quad (18)$$

$$r_{MO} = r_{H_2O} = k_2 c_{DAA} \quad (19)$$

where the rate constant k_1, k_{-1} and k_2 are listed in Table 3. The reaction to produce EC is represented by

$$EA + EO \xrightarrow{k} EC \quad (20)$$

The reaction rate for the formation of EC under CD conditions (excess of ethanol) is evaluated using the data measured by Xu et al. [29] as follows:

$$r_{EC} = 1.61 \times 10^8 \exp\left(\frac{63\,320}{RT} \right) c_{EO} \quad (21)$$

The activity coefficients for an equilibrium ratio of each component are computed by the modified UNIQUAC model [30]. The parameters for the UNIQUAC model have been provided by previous papers [19,31]. Other physical and chemical properties are estimated using the predictive methods recommended by Reid et al. [32].

3. Results and discussions

For the purpose of comparing the pseudo-homogeneous non-equilibrium and the three-phase non-equilibrium model for CD processes, a series of simulations were carried out on the synthesis of EC and DAA using the Newton–Raphson method to solve those models.

3.1. The synthesis of EC

The experiments were carried out in a 200 mm packed column. The molecular sieve NKC-01 catalyst spheres were placed inside a fiberglass bag, which was wrapped with demister wire and arranged in the reactive section of the column. The structural and operation parameters of the CD column were given in a previous paper [31]. We used the three-phase non-equilibrium model to simulate the EC process and compared with that from the pseudo-homogeneous non-equilibrium model. It was found that there is little difference in the predictions between these two models for the synthesis of EC via a CD process at a reflux ratio of 3 [31]. Here we change the reflux flow ratio to 2, similar predictions are also obtained for the two different models (Table 4).

The distinction between these two models lies in the treatment of liquid–solid mass and heat transfer. The

Table 4
Typical results from experiment and predictions for the synthesis of EC

Parameter	Measured	Predicted by a two-phase model	Predicted by a three-phase model
Temperature of top (K)	381.2	380.2	381.3
Temperature of reboiler (K)	444.2	441.4	443.9
Conversion of EO (%)	88.0	85.5	89.1
Selectivity of EC (%)	99.0	100	100
Feed ($kg\,h^{-1}$)	230	230	230
Bottom product ($kg\,h^{-1}$)	58	58	58
Reflux ratio	2	2	2
Bottom, mol fraction			
EA	0.01	0.045	0.021
EO	0.0	0.0	0.0
EC	0.98	0.955	0.979
Other ethers	0.01	0.0	0.0
Distillate, mol fraction			
EA	1.0	0.99	0.979
EO	0.0	0.01	0.021
EC	0.0	0.0	0.0

pseudo-homogeneous non-equilibrium model ignores the concentration and temperature gradients between the liquid and solid. However, it is not suitable for a reaction that is affected greatly by the mass and heat transfer between the liquid and solid. This is because the temperature and concentration on the catalyst surface should be very different from those in the liquid bulk under these circumstances. For the synthesis of EC via a CD process, it seems that the concentration and temperature gradients could be ignored. In addition, it is also likely that the production of EC is not greatly affected by the liquid–solid mass transfer. Therefore, it appears that for a reaction system that is kinetically controlled, a pseudo-homogeneous non-equilibrium model may be adequate for the simulation of a CD process.

3.2. The aldol condensation of Ac

The experiments were carried out at atmospheric pressure in a 25 mm column under total reflux. The Amberlite IRA-900 anion exchange resin catalyst filled in fibreglass bags and wrapped with demister wire was used in the experiments. The detailed experimental procedure and column specifications have been given by Podrebarac et al. [26]. The simulation results obtained from a three-phase non-equilibrium model have been presented in a previous paper [19].

Comparisons of the simulation results of the vapour composition, liquid composition and temperature profiles along the CD column from the three-phase non-equilibrium model and the pseudo-homogeneous non-equilibrium model are shown Figs. 3–5. Fig. 3 shows the composition profiles in the vapour phase for the pseudo-homogeneous and the three-phase non-equilibrium models. As expected from the boiling point differences Ac is concentrated at the top and products are found at the bottom of the column. However, the simulated composition profiles are very different in the catalytic reaction zone, the stripping section and in the reboiler for both models. Differences are also found in the liquid composition profiles predicted by both models as shown in Fig. 4. These results indicate the predictions of the formation rates of DAA, MO and water obtained from these two models are different. Fig. 5 displays the liquid temperature profiles calculated from those two models. It can be seen that the differences only occur in the stripping section and the reboiler. The pseudo-homogeneous non-equilibrium model predicts a lower temperature in the stripping section and a higher temperature in the reboiler. Therefore, the product compositions in the reboiler predicted by these two models should be very different. Under the given operating conditions the three-phase non-equilibrium model predicts that the product from the reboiler consists of 59 mol% Ac, 19.4 mol% DAA, 10.8 mol% MO, 10.8 mol% water. These predictions are in good agreement with the experimental data (60 mol% Ac, 19 mol% DAA, 10.5 mol% MO and 10.5 mol% water). However, the predictions from the pseudo-homogeneous non-equilibrium model (61.2 mol% Ac, 35.4 mol% DAA, 1.7 mol% MO and 1.7 mol% water) are far from the measured data. It is clear from Table 5 that there are significant differences in the simulation results obtained from the two different models for the DAA and MO productivities at reflux flow rate of 15.6, 16.3 and 22.9 g min^{-1}. It is interesting to note that only the three-phase non-equilibrium model could adequately simulate the CD process of the aldol condensation of Ac at reflux flow rates of 15.6, 16.3 and 22.9 g min^{-1}. These results indicate that the temperature and concentration gradients between liquid phase and catalyst surface could not be ignored at low reflux flow rates and hence there are significant differences between the two models. Another possibility is that multiple steady-states may be occurring in either one or both of the models under the conditions used for the simulation. Results of a bifurcation analysis [16] carried out using the reboiler duty as the independent parameter and the DAA mole fraction in the reboiler as the dependent parameter for both models are shown in Fig. 6. It can be

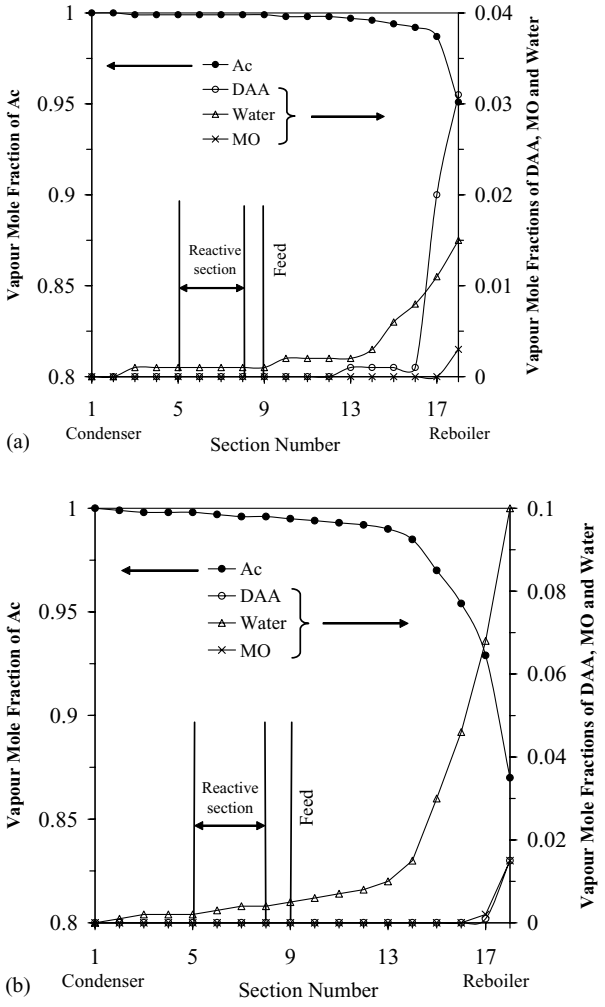

Fig. 3. Profiles of vapour composition along the column: (a) when the pseudo-homogeneous non-equilibrium model is used; (b) when the three-phase non-equilibrium model is used (catalyst, 131 ml; reflux, 16.3 g min^{-1}; feed, 152 ml h^{-1}).

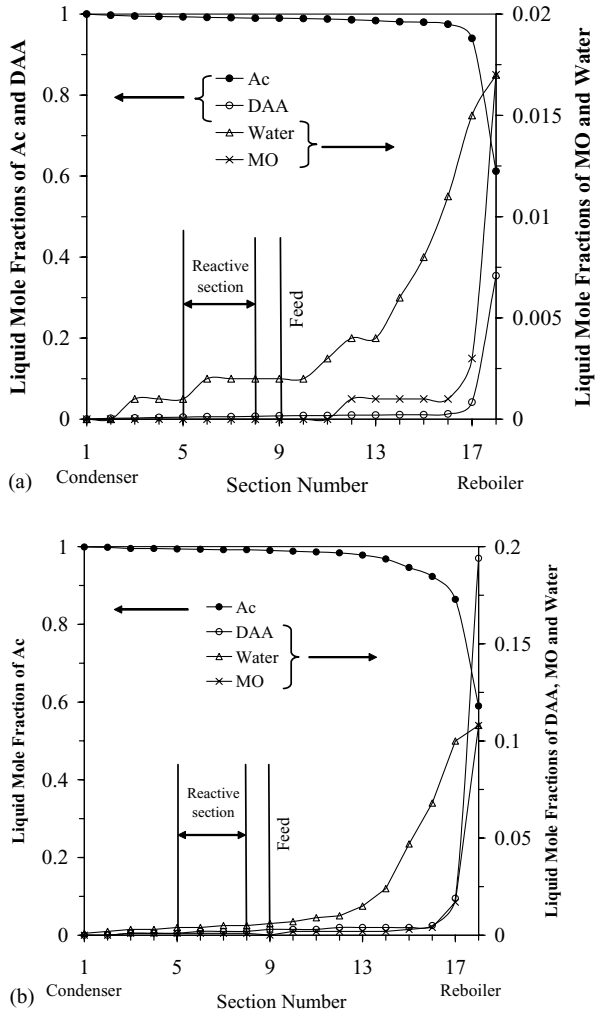

Fig. 4. Profiles of liquid composition along the column: (a) when the pseudo-homogeneous non-equilibrium model is used; (b) when the three-phase non-equilibrium model is used (catalyst, 131 ml; reflux, 16.3 g min^{-1}; feed, 152 ml h^{-1}).

seen that no steady-state multiplicity was found for both models over a range of reboiler duty. It is interesting to note in Fig. 6 that the pseudo-homogeneous model predicts a higher DAA mole fraction at reboiler duties less than 300 W and that at higher reboiler duties, both model predictions

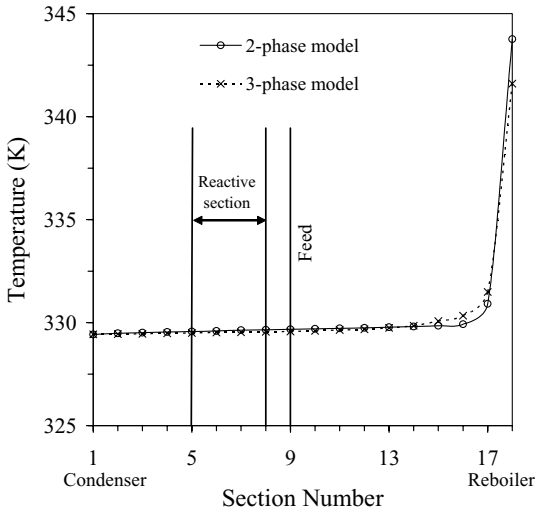

Fig. 5. Profiles of the liquid temperature along the column obtained from the pseudo-homogeneous and three-phase non-equilibrium models (catalyst, 131 ml; reflux, 16.3 g min^{-1}; feed, 152 ml h^{-1}).

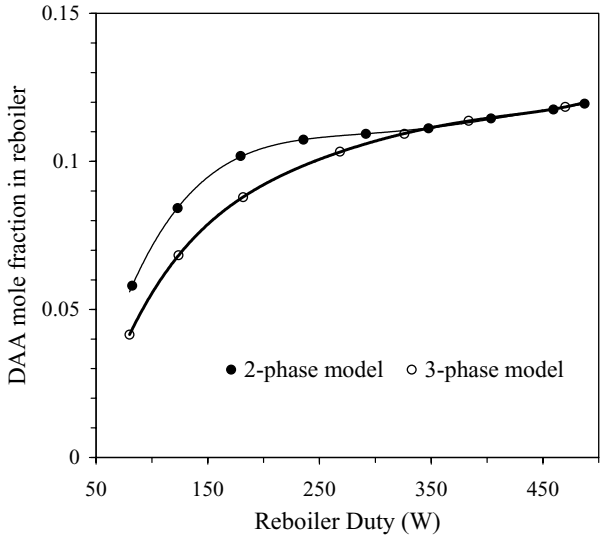

Fig. 6. Influence of reboiler duty on DAA concentration in the reboiler (catalyst, 131 ml; feed, 152 ml h^{-1}).

Table 5
Comparison of DAA and MO productivities between the experimental data and the model predictions

Catalyst (ml)	Reflux (g min^{-1})	Reboiler duty (W)	DAA productivity [g(ml-catalyst)$^{-1}$ h^{-1}]			MO productivity [g(ml-catalyst)$^{-1}$ h^{-1}]		
			Measured	Two-phase prediction	Three-phase prediction	Measured	Two-phase prediction	Three-phase prediction
43[a]	15.6	190	0.63	0.87	0.61	0.21	0.01	0.21
91[a]	22.9	250	0.49	0.58	0.50	0.14	0.10	0.14
131[a]	16.3	200	0.29	0.47	0.30	0.15	0.02	0.14
131[a]	30.0	320	0.46	0.46	0.46	0.14	0.14	0.15
43[b]	25.4	280	0.78	0.79	0.76	0.21	0.22	0.20

[a] Refers to catalyst I in Table 3.
[b] Refers to catalyst II in Table 3.

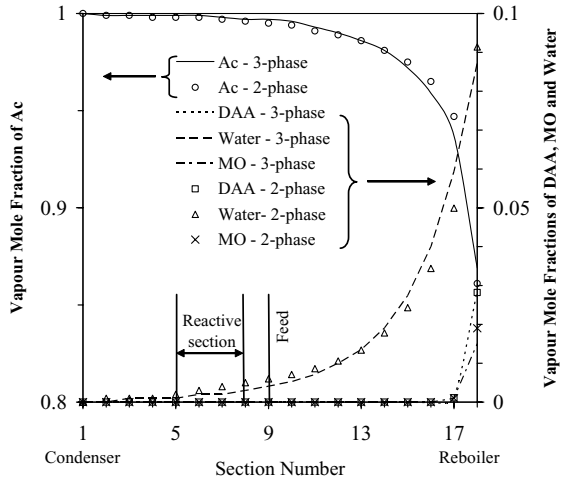

Fig. 7. Profiles of vapour composition along the column for both non-equilibrium models (catalyst, 131 ml; reflux, 30 g min^{-1}; feed, 152 ml h^{-1}).

for the DAA mole fraction in reboiler are the same. Indeed Table 5 shows that at reboiler duties of 280 W and 320 W, both model predictions for the DAA productivity and MO productivity agree with the experimental data.

Figs. 7 and 8 show the profiles of the vapour and liquid composition along the column at a reflux flow rate of 30 g min^{-1} (320 W) for both models. It is important to note that at the high reflux flow rate, both models predict essentially the same liquid and vapour composition along the whole length of the column in contrast to Figs. 3 and 4 where very different liquid and vapour composition are obtained at a low reflux flow rate of 16.3 g min^{-1} (200 W). These results clearly indicate that at low reflux flow rates, the production of DAA is mass transfer controlled and hence the pseudo-homogeneous non-equilibrium model overpredicts the production of DAA (Table 5, Fig. 6) as

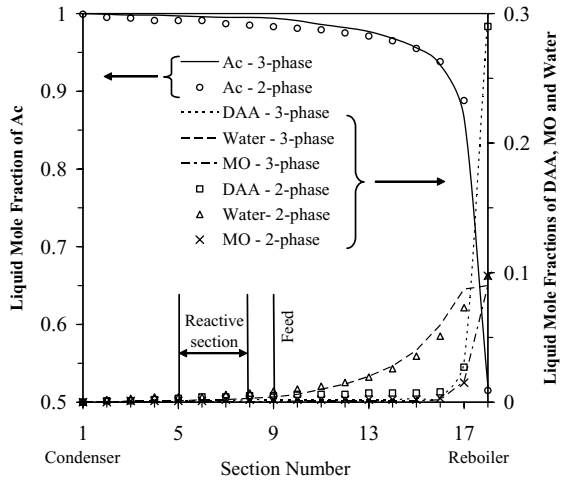

Fig. 8. Profiles of liquid composition along the column for both non-equilibrium models (catalyst, 131 ml; reflux, 30 g min^{-1}; feed, 152 ml h^{-1}).

it ignores the liquid–solid mass transfer resistance. Therefore a three-phase non-equilibrium model is required to simulate the productivity of DAA and MO under process conditions where the production of DAA is mass transfer controlled. We have previously reported that the production of DAA is limited by mass transfer resistance through the catalyst bags while the production of MO is kinetically controlled [18]. According to the process analysis for the production of DAA [20], the formations of DAA and MO are both kinetically controlled when the reflux flow rate is above 26 g min^{-1}. Therefore, predictions from a pseudo-homogeneous non-equilibrium model are in agreement with the experimental data for a reflux flow rate over 26 g min^{-1}, because the temperature and concentration gradients between liquid phase and catalyst surface could be ignored. However, there are substantial differences between the pseudo-homogeneous non-equilibrium and three-phase non-equilibrium model predictions when the productivity is limited by the liquid–solid mass transfer rate. Therefore our results indicate a three-phase non-equilibrium model is required to describe a CD process which is sensitive to liquid–solid mass transfer.

4. Conclusions

A comparison of the model predictions obtained from the three-phase non-equilibrium model and a pseudo-homogeneous non-equilibrium model has been carried out for the synthesis of EC and the aldol condensation of Ac via CD. For the synthesis of EC there is little difference in the predicted conversion and selectivity, at lease at the operation conditions, between a pseudo-homogeneous non-equilibrium model and a three-phase non-equilibrium model. In the aldol condensation of Ac, significant differences in the model predictions between a pseudo-homogeneous non-equilibrium model and a three-phase non-equilibrium model were found at low reflux flow rates when the CD process is significantly affected by solid–liquid mass transfer. Hence our results suggest that for a reaction system that is kinetically controlled, a pseudo-homogeneous non-equilibrium model may adequately simulate the temperature profile, yield and selectivity for a CD process. However, for a CD process that is sensitive to the solid–liquid mass transfer, a three-phase non-equilibrium model is required.

Acknowledgements

Financial support from Natural Sciences and Engineering Research Council of Canada is gratefully acknowledged.

References

[1] M. Malone, M.F. Doherty, Reactive distillation, Ind. Eng. Chem. Res. 39 (2000) 3953–3957.

[2] F.T.T. Ng, G.L. Rempel, Catalytic Distillation, in: Encyclopaedia of Catalysis, Wiley, New York, 2002.
[3] J.L. Bravo, A. Pyhalahti, H. Jarvelin, Investigations in a catalytic distillation pilot plant: vapor/liquid equilibrium, kinetics, and mass transfer issues, Ind. Eng. Chem. Res. 32 (1993) 2220–2225.
[4] A.A. Abufares, P.L. Douglas, Mathematical modelling and simulation of an MTBE catalytic distillation process using Speed Up and Aspen Plus, Trans. Inst. Chem. Eng. A 73 (1995) 3–12.
[5] Q. Smejkal, M. Šoóš, Comparison of computer simulation of reactive distillation using Aspen Plus and Hysys software, Chem. Eng. Process. 41 (2002) 413–418.
[6] J.A. Wesselingh, Non-equilibrium modeling of distillation, Trans. Inst. Chem. Eng. A 75 (1997) 529–538.
[7] J. Lee, M.P. Dudukovic, A comparison of the equilibrium and nonequilibrium model for a multicomponent reactive distillation column, Comput. Chem. Eng. 23 (1998) 159–172.
[8] R. Taylor, R. Krishna, Modelling reactive distillation, Chem. Eng. Sci. 55 (2000) 5183–5229.
[9] Y. Zheng, X. Xu, Study on catalytic distillation processes. Part II. Simulation of catalytic distillation processes—quasi-homogeneous and rate-based model, Trans. Inst. Chem. Eng. A 70 (1992) 465–470.
[10] M.G. Sneesby, M.O. Tadé, R. Datta, T.N. Smith, ETBE synthesis via reactive distillation. 1. Steady-state simulation and design aspects, Ind. Eng. Chem. Res. 36 (1997) 1855–1869.
[11] A.P. Higler, R. Taylor, R. Krishna, Modeling of a reactive separation process using a nonequilibrium stage model, Comput. Chem. Eng. 22 (1998) S111–118.
[12] R. Baur, R. Taylor, R. Krishna, Dynamic behaviour of reactive distillation columns described by a nonequilibrium stage model, Chem. Eng. Sci. 56 (2001) 2085–2102.
[13] A. Górak, A. Hoffmann, Catalytic distillation in structured packings: methyl acetate synthesis, Am. Inst. Chem. Eng. J. 47 (2001) 1067–1076.
[14] K. Sundmacher, U. Hoffmann, Development of a new catalytic distillation process for fuel ethers via a detailed nonequilibrium model, Chem. Eng. Sci. 51 (1996) 2359–2368.
[15] A.P. Higler, R. Taylor, R. Krishna, Nonequilibrium modeling of reactive distillation: a dusty fluid model for heterogeneously catalyzed processes, Ind. Eng. Chem. Res. 39 (2000) 1596–1607.
[16] R. Baur, R. Taylor, R. Krishna, Bifurcation analysis for TAME synthesis in a reactive distillation column: comparison of pseudo-homogeneous and heterogeneous reaction kinetics models, Chem. Eng. Process. 42 (2003) 211–221.
[17] C. Huang, L. Yang, F.T.T. Ng, G.L. Rempel, Application of catalytic distillation for the aldol condensation of acetone: a rate-based model in simulating the catalytic distillation performance under steady-state operations, Chem. Eng. Sci. 53 (1998) 3489–3499.
[18] C. Huang, F.T.T. Ng, G.L. Rempel, Application of catalytic distillation for the aldol condensation of acetone: the effect of the mass transfer and kinetic rates on the yield and selectivity, Chem. Eng. Sci. 55 (2000) 5919–5931.
[19] Y. Zheng, F.T.T. Ng, G.L. Rempel, Catalytic distillation: a three-phase nonequilibrium model for the simulation of the aldol condensation of acetone, Ind. Eng. Chem. Res. 40 (2001) 5342–5349.
[20] Y. Zheng, F.T.T. Ng, G.L. Rempel, Process analysis for the production of diacetone alcohol via catalytic distillation, Ind. Eng. Chem. Res. 42 (2003) 3962–3972.
[21] R. Taylor, R. Krishna, Multicomponent Mass Transfer, Wiley, New York, 1993.
[22] K. Onda, H. Takeuchi, Y. Okumoto, Mass transfer coefficients between gas and liquid phase in packed columns, J. Chem. Eng. Jpn. 1 (1968) 56–62.
[23] J.L. Bravo, J.R. Fair, Generalized correlation for mass transfer in packed distillation columns, Ind. Eng. Chem. Proc. Des. Dev. 21 (1982) 162–170.
[24] Y. Zheng, X. Xu, Study on catalytic distillation processes. Part I. Mass transfer characteristics in catalyst bed within the column, Trans. Inst. Chem. Eng. A 70 (1992) 459–464.
[25] C.J. King, Separation Processes, McGraw-Hill, New York, 1980.
[26] G.G. Podrebarac, F.T.T. Ng, G.L. Rempel, The production of diacetone alcohol with catalytic distillation. Part I. Catalytic distillation experiments, Chem. Eng. Sci. 53 (1998) 1067–1075.
[27] G.G. Podrebarac, F.T.T. Ng, G.L. Rempel, The production of diacetone alcohol with catalytic distillation. Part II. A rate-based catalytic distillation model for the reaction zone, Chem. Eng. Sci. 53 (1998) 1077–1088.
[28] G.G. Podrebarac, F.T.T. Ng, G.L. Rempel, A kinetic study of the aldol condensation of acetone using an anion exchange resin catalyst, Chem. Eng. Sci. 52 (1997) 2991–3002.
[29] X. Xu, W. Zhang, Y. Liu, W. Dong, Study on synthesis of cellosolve with catalytic distillation, Gaoxiao Huaxue Gongcheng Xuebao 4 (1990) 374–379.
[30] J. Prausnitz, T. Anderson, E. Grens, C. Eckert, R. Hsieh, J. O'connell, Computer Calculations for Multicomponent Vapor–Liquid and Liquid–Liquid Equilibria, Prentice-Hall, New Jersey, 1980.
[31] Y. Zheng, F.T.T. Ng, G.L. Rempel, Modeling of the catalytic distillation process for the synthesis of ethyl cellosolve using a three-phase nonequilibrium model, Int. J. Chem. Reactor Eng. 1 (2003) A4, http://www.bepress.com/ijcre/vol1/A4.
[32] R.C. Reid, J.M. Prausnitz, B.E. Poling, The Properties of Gases and Liquids, McGraw-Hill, New York, 1987.